A MICROFLUIDIC DEVICE FOR SORTING LIVER CANCER STEM CELL IN A CONTINUOUS BIOLOGICAL FLUID

M.W. WANG[1,c], K.S. JENG[2], M.C. YU[2], and J.C. SU[2]

[1]Department of Mechanical Engineering, Oriental Institute of Technology, New Taipei City 220, Taiwan
[2]Far-Eastern Memorial Hospital, New Taipei City 220, Taiwan

[c]Corresponding author: Tel.: +886277380145; Fax: +886277386648; Email: avian@mail.oit.edu.tw

KEYWORDS:
Main subjects: biological flows, flow visualization
Fluid: micro and nano-fluidics
Visualization method(s): classical optical methods
Other keywords: non-uniform electric fields, dielectrophoretic force

ABSTRACT: In order to make possible the selective sorting of hepatocellular carcinoma stem cells (CD133+ HCC SCs) in biofluids without to use an antigen-antibody reaction to attach antibody-immobilized nanobeads to the surfaces of HCC SCs. The unique dielectric properties of HCC SC has been tested and obtained by the applying AC electrical field with various frequency and strength between an planar microelectrodes. Eventually, the HCC SC can be manipulated and separated from the mixture by applying specific dielectrophoretic force dependent upon unique dielectric properties of HCC SCs. Creating the HCC SCs make this subsequent separation possible. To effect the actual separation, a micro channel with two dimensional electrodes has been designed on a Pyrex glass substrate and fabricated with micro fabrication technology. A local dielectrophoretic force, obtained from non-uniform electric fields, was used for manipulating the unique HCC SCs in a continuous flow. By the experimental studies that the homogenizered tumor cell specimens incur a local dielectrophoresis field when they are suspended in a continuous buffer fluid (flow velocity v = 0.1 cm/s) and exposed to RF electric fields at specific frequency (13.56 MHz). Using this device, the microchannel with planar microelectrodes provides a local dielectrophrosis field strong enough to manipulate the mobility of HCC SCs in a continuous biological fluid.

1 INTRODUCTION

Hepatocellular carcinoma (HCC) is the most common primary malignancy of the liver in adults. It is also the fifth most common solid cancer worldwide and the third leading cause of cancer-related death.[1] Current research supports that HCC derived from malignant transformation of hepatic progenitor cells (HPC). There may be at least three distinct cell lineages with progenitor cell properties susceptible to neoplastic transformation: hepatocyte, oval/hepatic progenitor cells, and bone marrow-derived stem cells. In hepatocarcinogenesis, multiple signaling transduction pathways, important for HCC stem cell (SC) proliferation and differentiations, are deregulated. Strategies are being developed to identify and characterize the liver cancer stem cells. Targeting liver cancer stem cells (HCC SCs) may bring hope to curing hepatocellular carcinoma. Identification of specific cell surface markers for each of the HPC types, production of corresponding monoclonal antibodies and cell sorting techniques have together revolutionized the characteristics of normal SCs.[2-6] Given the current problems in successfully treating HCC, we need to aim for novel therapeutic strategies. Understanding and unravelling the characteristics of SC biology in HCC may pave the way to such novel strategies.
In the form of components such as microchannels, micromixers and microseperators, micro-fluidic devices have been widely adopted for many kinds of biological and chemical applications.[7] Most of the chemical and biological reactions are performed in fluid with suspended cells. In order to make possible the selective sorting of specific cell in biofluids, the first step is to use a tissue cell homogenizer to decentralize the tumor tissue sections into the phosphate buffered saline (PBS). Later, the resulting HCC SCs must be trapped and separated from the mixture by applying other technologies. One of the fundamental difficulties in manipulating the HCC SCs is that most conventional operating tools are orders of magnitude larger than the HCC SCs, which range in size from a few nanometers to micrometers. An additional problem is that bio-fluid is an insulator of magnetism and electricity. A number of traditional methods utilized to manipulate the HCCSCs have their own limitations and disadvantages. Antibody-based magnetic sorting is among the most useful of such separation technologies, because it achieves rapid and thorough attachment of the

antibodies onto the specific target SCs.[8] Magnetic separation has also proven invaluable as a method for the pre-enrichment of complex samples.[9] However, magnetic selection strategies operate with only a single operating parameter (i.e., magnetism), and the development of similar methods capable of enriching multiple distinct species simultaneously has proven challenging.[10] Of all the micro-fluidic sorting technologies, the manipulation of biological particles by dielectrophoresis is probably the most broadly applied method.[11,12] A dipole movement is induced in the biological particles when they enter an AC field. In an asymmetrical electric field, the polarized particles incur a force that can induce them to move forward to regions of high or low potential field, depending on the polarizability of the particles compared with that of the suspending medium. This force was termed dielectrophoresis (DEP) by Pohl.[11,13] Thus by choosing a medium of appropriate conductivity and permittivity, particles of similar dielectric properties can be trapped efficiently. Recent studies have shown that submicron particles can be elegantly manipulated using dielectrophoretic methods. Leukemic cells,[14] breast cancer cells,[15] and CD34 SCs[16] can be sorted or enriched from human blood. Combined electrophoretic and dielectrophoretic forces have been used to trap and manipulate DNA on planar microelectrodes.[17-19] However, in the above mentioned studies, performance was restricted due to the fact that most of the manipulation and separation of submicron particles was performed in a steady pool. Performance in a continuous flow is better and more efficient. Furthermore, only a few experiments have been reported regarding the use of dielectrophoretic manipulation to trap and separate nanobead/stem cell compounds.[15, 20-23] Although the MT-DACS (Multiple Dielectrophoresis Activated Cell Sorter) has been developed and used to achieve multiple bacterial target cell separation, it is a complex electrodes structure that does not allow for the precise manipulation of hydrodynamic force.[20, 24, 25] For these reasons, we have conducted a detailed investigation of the mechanisms that enable the trapping of CD133+ HCC SCs by dielectrophoretic manipulation. The simple arrangement of planar microelectrodes that is required is regarded as a promising scheme for future biological studies.

To obtain an efficient sorting reaction and HCC SCs that can be sorted and separated from a continuous biological fluid flow, a microfluidic component of a microchannel with planar microelectrodes has been designed and fabricated by photolithographic process. A local dielectrophoretic force obtained from nonuniform electric fields was elected to manipulate and sort HCC SCs in a continuous BPS flow. The experimental studies indicate that the HCC SC undergoes weak positive dielectrophoresis and the normal HCC cell undergoes strong negetive dielectrophoresis when suspended in a continuous flow and exposed to RF/AC fields. Through this device, the sorting accuracy of HCC SCs is better than traditional magnetic selection strategy and up to 60% in a continuous flow was less than 0.1 cm/s, based on an applied power of $10V_{peak\text{-}peak}$ and a frequency of 13.56 MHz AC field. Under those circumstances, identification and sorting of HCC SCs can be achieved in a short time. Giving the current problems in successfully treating HCC, we can find novel therapeutic strategies. Understanding and unravelling the characteristics of SC biology in HCC pave the way to such novel strategies.

2 THEORETICAL MODEL

2.1 Dielectrophoresis force calculation

Previously, the classical dielectrophoretic model has been utilized for a spherical cell manipulation. In this work, due to the nature of the cell membrane and morphology, the classical spherical model must be modified in order to describe the polarization mechanics of real HCC SCs.[26] A real HCC SC can be described as an oblate sphere of highly conductive cytoplasm surrounded by a thick membrane. For a thick layer shell cell, the procedure is to start with the innermost sphere and the layer enclosing it, and to define an effective permittivity ε_c'. The thick layer shell cell is thus replaced by an equivalent, homogenous sphere with a radius equal to that of the outermost shell. As the CM factor, $K(\omega)$, used in the DEP force expression is valid only for homogeneous spherical cells, it is necessary to modify this factor taking into account both the spheroidal shape and low-conductive cell membrane of the HCC SC. Irimajiri[27] had modified a model with a multi-shelled Maxwell-Wagner (MW) theory in order to approximate the dielectric polarization of biological cells suspended in an electrolyte solution. Here, we better approximate the biconcave shape of a liver stem cell as an oblate spheroid. For the case a single-shell oblate spheroid with major axis aligned parallel with the applied field, the CM factor can be shown to be $K(\omega)_{MW} = V_c \varepsilon_m (\varepsilon_c'-\varepsilon_m^*) / [(\varepsilon_c'-\varepsilon_m^*) A_{op}+\varepsilon_m^*]$. The parameter A_{op} describes the geometry specific degree to which the exterior of the cell, from the outer membrane edge to infinity, depolarizes along the principal axis, V_c represents the cell volume, and ε_c' is the effective permittivity of the cell given by $\varepsilon_c' = \varepsilon^*_{mem} \{\varepsilon^*_{mem} +(\varepsilon^*_{cyto} - \varepsilon^*_{mem})[A_{ip} +v(1- A_{op})]\} / \{\varepsilon^*_{mem} +(\varepsilon^*_{cyto} - \varepsilon^*_{mem})[A_{ip} - vA_{op}]\}$, where ε^*_{mem} and ε^*_{cyto} are the complex permittivity's of the cell membrane and cytoplasm, respectively, A_{ip} describes the depolarization from just the membrane to infinity, v (which is $v = r^2c / [(r + d)^2 (c + d)]$) is the volume ratio of the cell exterior to interior, r the cell radius, c the cell half-length, and d is the membrane thickness. In the case of an erythrocyte cell, d is approximately three orders of magnitude less than r and c, and thus the approximation that $A_{op} = A_{ip}$ can be made, and a useful

expansion of this factor can be expressed in terms of $\gamma = c/r$ as $A_{op} = A_{ip} = \{1+[3(1-\gamma^{-2})/5]+ [3(1-\gamma^{-2})^2/7]+ \ldots\} / 3\gamma^{-2}$. For a sphere particle, $\gamma = 1$, and thus $A_{op} = A_{ip} = 1/3$, which forces this model to converge to the well known spherical CM factor. However, γ does not equal unity for a liver stem cell, and unless otherwise stated, the time-averaged dielectrophoretic force acting a cell is give by the single-shelled MW theory, $F_{DEP} = (2/3)\pi r^2 c\varepsilon_m \mathrm{Re}\{V_c\, \varepsilon_m (\varepsilon_c'-\varepsilon_m^*) / [(\varepsilon_c'-\varepsilon_m^*) A_{op}+\varepsilon_m^*]\} \nabla|E_{rms}|^2 = (2/3)\pi r^2 c\varepsilon_m \mathrm{Re}\{K(\omega)_{MW}\} \nabla|E_{rms}|^2$ where r is the radius of the cell, c the cell half-length, E_{rms} the root mean square value of the electric field, and $\mathrm{Re}\{K(\omega)_{MW}\}$ is the real part of modified CM factor. Base on the theoretical model of dielectrophoresis, the dielectrophoretic responses of HCC SCs are governed by the real part of the Clausius-Mossotti (CM) factor. In other words, the responses of HCC SCs are predominated by conductivity and permittivity. The HCC SC is bigger than serum for the permittivity ($\varepsilon_c > \varepsilon_m$) and the conductivity ($\sigma_m > \sigma_c$). Then the cells will be attracted to electric field intensity maxima at suitable frequencies The frequency-dependent behavior of normal HCC cells reverses if $\varepsilon_{c'} > \varepsilon_{m'}$ and $\sigma_{c'} > \sigma_{m'}$.

The hydrodynamic drag force F_{drag} experienced by a HCC SC can be approximated as a spheroid translating relative to surrounding fluid with velocity v, using Stokes' drag for low Reynolds number flow $F_{drag} = -\zeta v$, where ζ is the friction factor of the HCC SC.[28] The friction factor for a homogeneous HCC SC is given by $\zeta = 6\pi\mu r K'$, where μ is the viscosity of the PBS medium and $K' = 8(1-\gamma^2) / 3\{\{[(2\gamma^2-3)/(1-\gamma^2)^{1/2}] \tan^{-1}(\gamma^{-2}-1)\}- \gamma^{-2}\}$ is the modify factor by taking into the spheroidal shape. For a sphere particle, $\gamma = 1$, and thus $K' = 1$, which forces this model to converge to the well known Stokes drag factor. Ignoring Brownian motion and buoyancy force, the equation of motion can be written as $m \cdot [dv/dt] = F_{DEP} - F_{drag}$. The moving velocities of the erythrocyte should be proportioned to the time-averaged dielectrophoretic force, so as $U = F_{DEP} / \zeta$ in the direction of $\nabla|E_{rms}|^2$.

2.2 Electric charging operation

The dielectrophoretic mobility of a cell scales directly with its surface area, so that to manipulate erythrocytes, high intensity electric field gradients are required. The high intensity electric field gradients associated with dielectrophoresis will create non-uniform temperature fields. Permittivity and conductivity are functions of temperature. Therefore, the spatially varying temperature field creates spatially varying permittivity and conductivity fields in the medium.[29] An applied electric field, coupled with spatial variations in permittivity and conductivity, creates inhomogeneous Coulomb and dielectric body forces in medium. This phenomenon will induce microscale medium motion and non-invasively stirring the medium at microscale.

According to the formula $W=\sigma E^2$, the power per unit volume of the electrical field that is absorbed by the serum medium is due to Joule heating.[26] The temperature of the serum medium can be calculated by solving the heat equation with a source term for electrical heat generation: $\rho_m c_p [(\partial T/\partial t) + U\cdot\nabla T] = k\nabla^2 T + \sigma E^2$, where U is the velocity, T is the temperature, ρ_m is the mass density, c_p is the specific heat at constant pressure, k is the thermal conductivity, and σ is the electrical conductivity of the serum medium. Temperature dispersion in the continuous flow is affected by advection: the heat equation can be shown as $U\cdot\nabla T = \alpha\nabla^2 T + (\sigma E^2/\rho_m c_p)$.

3 EXPERIMENTAL PROCEDURE

3.1 Preparation of HCC cell specimen

The study protocol was approved by and performed in accordance with the Committee of the Teaching and Research at the Far-Eastern Memorial Hospital. The HCC cells were either injected subcutaneously or intrahepatically into mice. Mice were killed between 3 and 6 months post injection, at which time tumors were harvested for further examination. Those mice injected with tumor cells but with no sign of tumor burden were generally terminated 5 months after tumor cell inoculation, and mice were opened up at the injection sites to confirm that there was no tumor development. Xenograft tumors were minced into 1-mm^3 pieces and incubated with tissue cell homogenizer for 20 minutes at 37°C under constant rotating conditions. The HCC cell suspension was obtained by filtering the supernatant through a 100μm and 40μm cell strainer (BD Biosciences). A specimen was decentralized into the phosphate buffered saline (PBS) for next sorting experiment.

3.2 Setup of flow visualization

For clear probing HCC cells fluidic transport, a high-power infrared radiation illuminated imaging flow visualization system with a long working distance objective-imaging system was set to measure the path of a microfluid flow inside the microfluidic device.[30] The fluid was driven by pressurized air and regulated by precise valves. A microflow meter is used for measuring flow rate. An infrared radiation diode laser (720-1024 nm, 10W) applied to illuminate the microfluidic chamber. Clear-cut cell images were captured using a camera via a dark field filter equipped with objective lens (M plan Apo Series M=100, numerical aperture NA = 0.42). In order to achieve high speed frame rates and obtain high-quality images, the camera was equipped with a complementary metal-oxide-semiconductor (CMOS) image sensor and a high-performance processor (1k×1k pixels, 12-bit grayscale, and 5000 frames/s, Fastcam SA1, Photron Ltd., Japan) that offered an outstanding light sensitivity and a high image quality that relies on USB2.0 connected to a PC. Its resolution and decay time were 32l p/mm and 2μs, respectively. In this work, a filtered illuminant with a wavelength of λ = 860 nm was used to display the cells flow; the diameter of cell ($d_c \approx$ 20-30 μm) was larger than the wavelength of illuminant, i.e., $d_c > \lambda$. In this regime, it is easy to image the HCC cells using normal elastic scattering techniques. For best results, the rule of thumb in setting the axial distance between slices is to have this distance equal to the Rayleigh depth of field (DOF), as given by the following equation: $DOF = \lambda / \{4\eta \sin^2 [0.5 \sin^{-1} (NA/\eta)]\}$, where λ is the wavelength, η is the refractive index of the medium (1.0 for air), and NA is the numerical aperture of the objective lens.[31] Therefore, the *DOF* was calculated to be about 8 μm.

3.3 Microfluidic device

The microfluidic device with the microelectrodes shown in figure 1 was fabricated by bonding a polydimethyl siloxane (PDMS) replica and a Pyrex glass chip. The cross-sectional average size and streamwise length of the channel were 500×300 μm^2 and 5 mm (W×H×L), respectively. In the fabrication of the PDMS replica, a microstereo lithography (μ-SLA) system rapidly directs the focused radiation of an appropriate power onto the surface of a liquid photopolymer resin, forming patterns of the solidified photopolymer. The feature size of the fragment is determined by the diameter of the focused laser spot on the photopolymer surface.[32] After forming, the master was cleaned with alcohol and deionized water for the easy removal of the PDMS replica from the master after curing. The prepolymer of PDMS and a curing agent were mixed at the ratio of 10:1 and then degassed in a vacuum chamber. The polymer mixture was poured onto the master, and then cured at 65℃ for 1 hr. After cooling, the PDMS replica was peeled off from the master. In accordance with the lithography techniques, the symmetric curvilinear microelectrodes, 200 Å Cr and 1000 Å Au, were deposited on the surface of the Pyrex glass using a magnetism DC sputtering coater, which provided precise and fast electrodes formation. The microfluidic device will connect to an AC power with 13.65MHz frequency and performance 10 $V_{peak\text{-}peak}$ (Agilent 33220 Function Generator), and the maximum electric field should occur in the vicinity of the tips of saw microelectrodes. The range of gap between opposing electrodes was smaller than the width of the flow channel in order to limit the flow range of separated polluted erythrocytes across the flow section. Then, the PDMS replica was oxidized in the O_2 plasma cleaner to achieve an interface bonding, and finally the replica was attached to the Pyrex glass chip. The microfuidic device was performed in a low flow speed (v = 0.1 cm/s) and then the pressure gradient is less than 0.02 kg/cm^2 in the channel. Therefore, the bonding interface between the PDMS replica and electrodes array is thus strong enough to prevent the leakage during the experiments.

3.4 Method to probe the HCC SCs

Traditional HCC SCs sorting, cells were labeled with CD133+ magnetic microbeads and sorted using the Miltenyi Biotec CD133 Cell Isolation Kit. In this study, we performed flow cytometry analyses of HCC SCs, cells were stained with PE-conjugated anti-human CD133+ (Miltenyi Biotec). Isotype-matched mouse immunoglobulins served as controls. Samples were analyzed and sorted on a BD FACSVantage SE (BD Biosciences).

4 Results and Discussion

4.1 Electric field simulation

The electric fields were modeled using ANSOFT™ Maxwell 3D, a finite element software package, to solve the electromagnetic problem. A two-dimensional model was sufficient to describe the electric fields of asymmetrical saw microelectrodes. To simplify, the system was modeled as if surrounded by PDMS. Figure 2 shows an ANSOFT Maxwell simulation of the electric field distribution generated by microelectrodes containing saw features. We can assure that the electric field gradient is at its maximum in the regions closest to the tips of asymmetric saw microelectrodes; HCC SCs and normal HCC cells can be separated in these regions.

4.2 Dielectrophoretic force calculation

The dielectrophoretic response of the HCC SC is governed by the Clausius-Mossotti factor. For biological cell the response is dominated by the cell conductivity, which in turn is governed by the surface charge on the cell. The conductivity of a HCC SC can be written as the sum of bulk and surface conductivity of cells, $\sigma=\sigma_{bulk} + (2K_{surface} / r)$,[33] where $K_{surface}$ is the surface conductance and σ_{bulk} is the bulk conductivity. The polarizability and the dielectrophoretic force on each SC can be calculated on the basis of the modified dielectrophoretic theory and the Stokes law mentioned above. Besides, this work describes a high frequency operation, $\omega = 13.56$ MHz, and thus alternative electric field induces a thick membrane potential will be reduced at a stable electrical field. The change of thick membrane conductivity in the medium can therefore be estimated.[34, 35] Figure 3 shows the frequency dependence of the modified Clausius-Mossotti factor for the HCC SC (the cell radius $r \approx$ 20-30 μm, cell half-length $c \approx$ 10-15 μm, and membrane thickness $d \approx$ 6-8 μm) and normal HCC cell (the cell radius $r \approx$ 10-20 μm, cell half-length $c \approx$ 5-10 μm, and membrane thickness $d \approx$ 0.2-0.8 μm) with a normal HCC cell permittivity $\varepsilon_{c'} \approx 2.56$, HCC SC permittivity $\varepsilon_c \approx 60$, a PBS medium permittivity $\varepsilon_m \approx 53$, a HCC SC conductivity $\sigma_c \approx 1.381$ Sm^{-1}, a normal HCC cell $\sigma_{c'} \approx 0.312$ Sm^{-1}, and a PBS medium conductivity $\sigma_m \approx 1.24$ Sm^{-1}.[36, 37] At same medium conductivity, it can be seen that in the frequency of 13.65MHz, the force on the normal HCC cell remains strong negative, whereas for HCC SC remains weak positive, so that the two HCC cell types respond in completely different directions to the electric field, with normal HCC cell experiencing negative DEP and HCC SC experiencing positive DEP, implying that the spatial separation of the two species should be possible in a continuous biological flow.

4.3 Additional forces effect

The actual electric field generated in a stasis medium fluid will induce high Joule heating, which leads to a rapid temperature rise and induces fluid flow. Local temperature variations in the stasis liquid will also bring about permittivity and conductivity inhomogeneities in the medium, which will produce a force to activate the medium fluid.[38] Rather than focus in the traditional manner on aspects of cells trapped in a static medium, this project is primarily concerned with the way continuous fluidic flow evokes rapid heat dispersion followed by a continuous flow.

According to the simplified heat transfer equation $U \cdot \nabla T = (k / \rho_m c_p) \nabla^2 T + (\sigma E^2 / \rho_m c_p)$, the change of temperature in the fluid, induced by advection in the continuous flow, can be estimated as $\Delta T_{adv} \sim \sigma V^2 / \rho_m c_p U$. The number is bigger than that of conduction $\Delta T_{cond} \sim \sigma V^2 / k$. For the PBS medium conductivity $\sigma_m = 1.24$ Sm^{-1}, $\rho_m = 1.001 \times 10^3$ kg/m^3, $c_p = 4.182$ kJ/kg . K, V=10V_{pp}, U = 0.1 cm/s, k =0.6W/m . K, the order analysis is $\Delta T_{cond} \sim O(2)$ and $\Delta T_{adv} \sim O(-1)$, and small gradients in temperature produce smaller gradients in permittivity and conductivity in the medium fluid. According to the results in a stasis medium, the change of temperature in the fluid approximates 10℃ so that the change of temperature in the continuous fluid should be less than 1℃. A general expression of the electrical force per unit volume on an imcompressible liquid is $F_{DEP\ net} = F_{DEP} - F_{electro\text{-}thermal}$, and $F_{electro\text{-}thermal} = E_{rms}^2 (1/\varepsilon)(\partial \varepsilon / \partial T)/2$ [39] Since the continuous flow does not increase instantaneously in response to the increased temperature, the electro-thermal force will have a minimal effect on continuous flow.

4.4 Dielectrophoretic manipulation

The observations indicate the conditions under which a HCC SC and normal HCC cell separation can be obtained. At suitable frequency and applied potential, it was possible to provide a local dielectrophrosis field strong enough to spatially manipulate and separate a mixture of HCC SCs and normal HCC cells into two distinct direction in a continuous biological flow (flow velocity v = 0.1 cm/s). This can clearly be observed in figure 4, which indicates the conditions under which HCC SCs sort can be achieved at an applied power 10 $V_{peak\text{-}peak}$. At a PBS medium conductivity of 1.24 Sm^{-1} and frequency of 13.56 MHz, the normal HCC cells experience a strong negative dielectrophoretic field, so that the normal HCC cells move toward the direction of sidewall in the biological fluid flow where the dielectrophoretic force is weakness. Relatively, the HCC SC experiences weak positive dielectrophoretic field, so that the SCs still moves toward the direction of downstream in the central of main fluid flow where the dielectrophoretic force is strong. The images show that the HCC SCs are steady moving in the central of the medium flow, and the normal HCC cells flow out of the central region of tips of the asymmetric saw microelectrodes. The moving velocity of normal HCC cells should be proportional to the time-averaged dielectrophoretic force, $U = F_{DEP}/\xi$, then $U_c = (2/3)\pi r^2 c \varepsilon_m \mathrm{Re}\{K(\omega)_{MW}\} \nabla |E_{rms}|^2 / (6\pi\mu r_{eff} K')$ (r_{eff} described a sphere of equivalent radius $r_{eff} = (r^2 c)^{1/3}$, K' is the modify friction factor $K' = 8(1-\gamma^2) / 3\{\{[(2\gamma^2-3)/(1-\gamma^2)^{1/2}] \tan^{-1}(\gamma^{-2}-1)\} - \gamma^{-2}\}$ for an oblate spheroid in the direction of $\nabla |E_{rms}|^2$.

Considering the steady-state condition, and neglecting the electro-thermal effect in a continuous flow, the deviation angle of normal HCC cells mobility with AC electric field application can be estimated as $\theta \sim \tan^{-1}[U_{DEP}/U_{flow}]$, where U_{flow} is the velocity of continuous flow and U_{DEP} is the DEP deviating velocity of cells (Fig. 5). By analyzing the theory, $U_{DEP}/U_{flow} \sim L_c/L_{flow}$ in constant time, the deviating angle can be conveyed to $\theta_c \sim \tan^{-1}[L_c/L_{flow}]$, where L_c =100 μm is the distance from the central flow to the center of electrodes. The range of dielectrophoresis field provided by the electrodes are L = 120 μm along the direction of downstream flow. Results of the deviation angles θ_c can be determined to be about 35 deg under the steady state. The approximate deviation angle θ_c is 30-40 deg determined through the experimental measurement, owing to the fact that the normal HCC cells are widely distributed in the both side regions of the asymmetric microelectrodes near the sidewalls of channel. The real positions of deviating normal HCC cells (Fig. 5) show that, for the real cases of flow considered here, the experiments and theoretical predictions have some similarities. The experimental measurements deviating from the theoretical prediction were attributed to the normal HCC cells that keep moving and slipping near the sidewall of flow channel in the continuous flow even though the normal HCC cells were repelled to the negative DEP force from electrodes. Under above reported operating conditions, we found our device is well suited for the sorting of HCC SCs in a continuous operation. Flow cytometry histogram analysis revealed that, after a single through the microfluidic device, the population in the outlet consisted of 65% CD133+ SCs. (Fig. 6)

5 Concluding Remarks

This study shows that HCC SCs can be sorted and separated by a suitable local dielectrophoretic force in a continuous biological flow. Local dielectrophoretic forces obtained from nonuniform electric fields were used to sort the HCC SCs. With an appropriate array of microelectrodes, a suitable electric field, the right frequency and medium flow velocity, HCC SCs can be sorted and separated out from a continuous biological flow. From the data, to sort and separate HCC SCs from specimen, the most effective driving velocity for the bloodstream flow was set at less than 0.1 cm/s through our microfluidic DEP device, based on an applied power of $10V_{peak\text{-}peak}$ and a frequency of 13.56 MHz AC field. This work demonstrates using DEP manipulating techniques for efficient sorting of unique cells within a medium may potentially allow biological sorting and separating to be performed relatively cheap and fast.

Acknowledge

The author thanks Far Eastern Memorial Hospital for the preparation and detection of the HCC cells specimen. Financial support from the Far Eastern Memorial Hospital, Oriental Institute of Technology and National Science Council (NSC100-2221-E-161-008-MY2) of R.O.C. (Taiwan) is greatly appreciated.

References

1. J. M. Llovet, A. Burroughs, J. Bruix *Hepatocellular carcinoma.* Lancet 2003, 362, p.1907.
2. S. Ma, K. W. Chan, L. Hu et al. *Identification and characterization of tumorigenic liver cancer stem/progenitor cells* Gastroenterology 2007, 132 (7), p.2542.
3. Z. F. Yang, P. Ngai, D. W. Ho et al. *Identification of local and circulating cancer stem cells in human liver cancer* Hepatology 2008, 47, p.919.
4. T. Yamashita, M. Forgues, W. Wang et al. *EpCAM and α-fetoprotein expression defines novel prognostic subtypes of hepatocellular carcinoma* Cancer Research 2008, 68 (5), p.1451.
5. T. Chiba, K. Kita, Y. W. Zheng et al. *Side population purified from hepatocellular carcinoma cells harbors cancer stem cell-like properties* Hepatology 2006, 44, p.240.
6. N.G. Green, A. Ramos, H. Morgan et al. *AC electrokinetics: a survey of sub-micrometre particle dynamics* J. Phys. D: Appl. Phys. 2000, 33, p.632.
7. S. Miltenyi, W. Muller, W. Weichel, A. Radbruch et al. *High gradient cell separation with MACS.* Cytometry 1990, 11, p.231.
8. L.A. Herzenberg, D. Parks, B. Sahaf, O. Perez, M. Roedereret et al. *The history and future of the fluorescence activated cell sorter and flow cytometry: a view from Stanford* Clin. Chem. 2002, 48, p.1819.
9. X.Y. Hu, P.H. Bessette, J.R. Qian, C.D. Meinhart, P.S. Daugherty, H.T. Soh et al. *Marker-specific sorting of rare cells using dielectrophoresis* Proc. Natl. Acad. Sci. U.S.A. 2005, 102, p.15757.
10. H.A. Pohl, *Dielectrophoresis*, (Cambridge University Press, Cambridge, U.K., 1987.
11. T. B. Jones, *Dielectromechanics*, Cambridge University Press, Cambridge, U.K., 1995.
12. H.A. Pohl *The Motion and Precipitation of Suspensoids in Divergent Electric Fields* J. Appl. Phys.1951, 22,

p.869.
13. F.F. Becker, X.B. Wang, Y. Huang, R. Pethig, J. Vykoukal, P.R.C. Gascoyne et al. *The removal of human leukaemia cells from blood using interdigitated microelectrodes* J. Phys. D: Appl. Phys. 1994, 27, p.2659.
14. F.F. Becker, X.B. Wang, Y. Huang, R. Pethig, J. Vykoukal, P.R.C. Gascoyne et al. *Separation of human breast cancer cells from blood by differential dielectric affinity* Proc. Natl. Acad. Sci. U.S.A. 1995, 92, p.860.
15. M. Stephens, M.S. Talary, R. Pethig, A.K. Burnett, K.I. Mills et al. *The dielectrophoretic enrichment of CD341 cells from peripheral blood stem-cell harvests* Bone Marrow Transplant 1996, 18, p.777.
16. M. Washizu and O. Kurosawa *Electrostatic manipulation of DNA in microfabricated structures* IEEE Trans. Ind. Appl. 1990, 26, p.1165.
17. M. Washizu, O. Kurosawa, I. Arai, S. Suzuki, N. Shimamoto et al. *Applications of electrostatic stretch-and-positioning of DNA* IEEE Trans. Ind. Appl. 1995, 31, p.447.
18. C.L. Asbury and G. van den Engh *Trapping of DNA in nonuniform oscillating electric fields* Biophys. J. 1998, 74, p.1024.
19. U. Seger, S. Gawad, R. Jogann, A. Bertsch, P. Renaud et al. *Cell immersion and cell dipping in microfluidic devices* Lab Chip 2004, 4, p.148.
20. U. Kim, J. Qian, S.A. Kenrick, P.S. Daugherty, H.T. Soh et al. *Mulit-Target Dielectrophoresis Activated Cell Sorter (MT-DACS)* Anal. Chem. 2008, 80, p.8656.
21. P.H. Bessette, X.Y. Hu, H.T. Soh, P.S. Daugherty et al. *Microfluidic Library Screening for Mapping Antibody Epitopes* Anal. Chem. 2007, 79, p.2174.
22. U. Kim, C.W. Shu, K.Y. Dane, P.S. Daugherty, J.Y.J. Wang, H.T. Soh et al. *Selection of Mammalian Cells According to Their Cell-Cycle Phase using Dielectrophoresis* Proc. Natl. Acad. Sci. U.S.A. 2007, 104, p.20708.
23. J.G. Kralj, M.T.W. Lis, M.A. Schmidt, K.F. Jensen et al. *Continuous dielectrophoretic size-based particle sorting* Anal. Chem. 2006, 78, p.5019.
24. P.R.C. Gascoyne and Vykoukal *Particle separation by dielectrophoresis* J. Electrophoresis 2002, 23, p.1973.
25. T. W. Hoeber, R. M. Hochmuth *Measurement of red cell modulus of elasticity by in vitro and model cell experiments* Mech. Eng. 1970, 92, p.604.
26. A. Irimajiri, T. Hanai, A. Inouye *A dielectric theory of "multi-stratified shell" model with its application to a lymphoma cell* J. Theor. Biol. 1979, 98, p.251.
27. Y. S. Lai, L .F. Mockros *The Stokes-flow drag on prolate and oblate spheroids during axial translatory acceleration* J. Fluid Mech. 1972, 52, p.1.
28. A. Ramos, H. Morgan, N.G. Green, A. Castellanos *AC Electrokinetics : A review of forces in microelectrode structure* J. Phys. D 1998, 31, p.2338.
29. M. W. Wang *Using dielectrophoresis to trap nanobead/stem cell compounds in continuous flow*. J. Electrochemical Soc. 2009, 156, p.G97.
30. S. Inouě, K. Spring, Microscope Image Formation. In “Video Microscope: The Fundamentals,” (Plenum Press: NY, U.S., 1997).
31. M. W. Wang, K. H. Teng *The Features of DVD-RAM Stamper Studies via Laser Energy Adjustment* Jpn. J. Appl. Phys. 2005, 44, p.2021.
32. W. M. Arnold, H. P. Schwan, U. Zimmermann *Surface conduc- tance and other properties of latex particles measured by electro-ro- tation* J. Phys. Chem. 1987, 91, p.5093.
33. I. Tuval, I. Mezić, F. Bottausci, Y. T. Zhang, N. C. MacDonald, O. Piro *Control of particles in microelectrode devices* Phys. Rev. Lett. 2005 , 95, 203903 p.1.
34. U. Zimmermann, G. A. Neil, *Electromanipulation of Cells*, (CRC Press: Boca Raton, F.L., 1996).
35. C. Balan, C. Balut, L. Gheorghe, C. Gheorghe, E. Gheorghiu, G. Ursu *Experimental determination of blood permittivity and conductivity in simple shear flow* Hemorheology and Microcirculation 2004, 30, p.359.
36. P. Gascoyne, J. Satayavivad, M. Ruchirawat *Microfluidic approaches to malaria detection Acta. Trop.* 2004, 89, p.357.
37. T. Heida, W. L. C. Rutten, E. Marani *Understanding dielectrophoretic trapping of neuronal cells: modeling electric field, electrode-liquid interface and fluid flow* J. Phys. D: Appl. Phys. 2002, 35, p.1592.
38. A. Ramos, H. Morgan, N. G. Green, A. Castellanos *Ac electrokinetics: a review of forces in microelectrode structures* J. Phys. D: Appl. Phys. 1998, 31, p.2338.

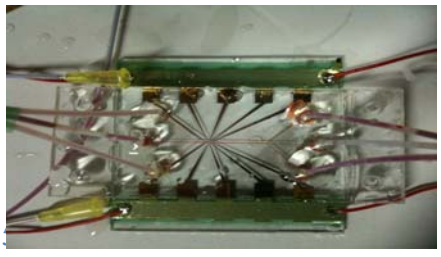

Figure 1 A microfluidic device with microelectrodes was fabricated by bonding a PDMS replica and a Pyrex glass chip.

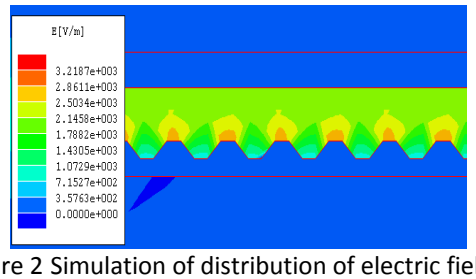

Figure 2 Simulation of distribution of electric field generated by asymmetric saw microelectrodes in a micro-channel.

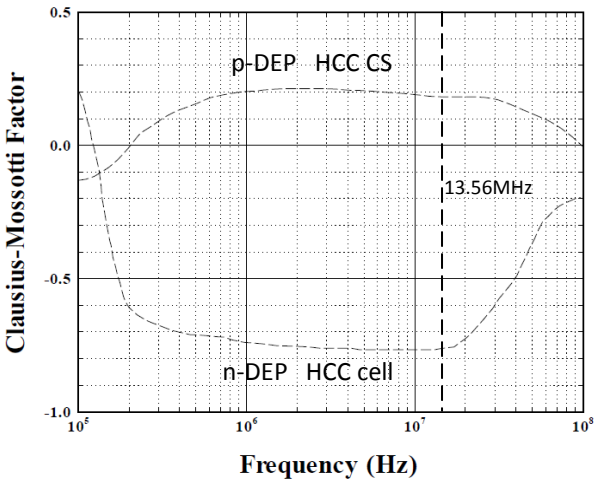

Figure 3 Frequency dependence of the Clausius-Mossotti factor (CM Factor) for the HCC cells.

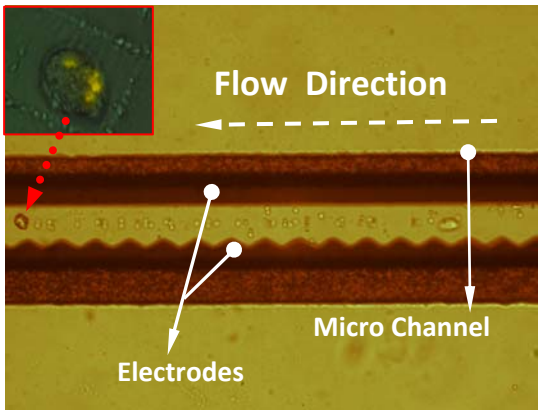

Figure 4 A microchannel with asymmetric plane electrodes provide a strong local dielectrophrosis field to sort the cancer stem cells in a continuous biofluid flow.

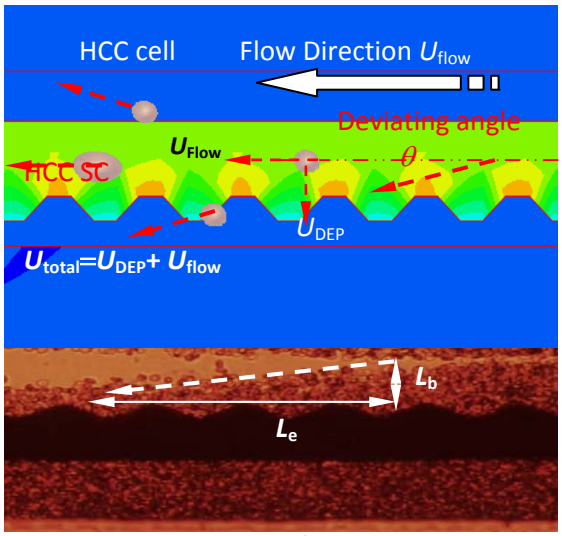

Figure 5 Deviation angle of the normal HCC cells flowing in the micro channel, $\theta \sim \tan^{-1}[U_{DEP}/U_{flow}] \sim \tan^{-1}[L_c/L_e]$.

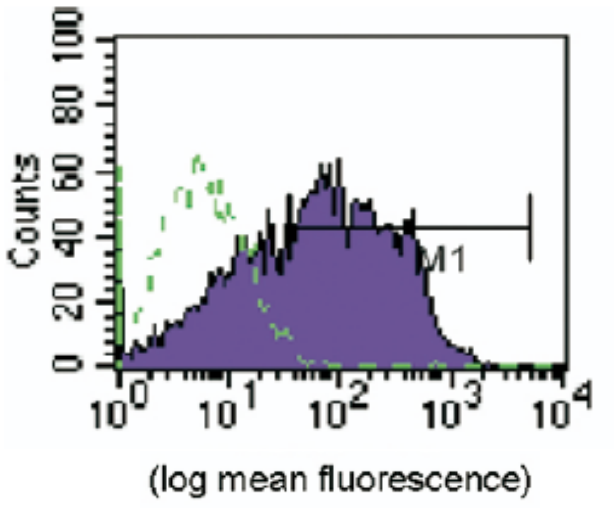

Figure 6 Flow cytometry histogram analysis.